Supporting information

Oxygen Redox Activities Governing High-Voltage Charging Reversibility of Ni-Rich Layered Cathodes

Table of contents

Materials and Methods

General characterizations (ICP-AES, XRD, ND, SEM)

All cathode materials (NR60, NR70, NR70-Al, NR90, NR90-Al) used in this work are provided by LG Energy Solution. The ICP-AES results were collected with a PerkinElmer OPTIMA 8300 ICP mass spectrometer installed at the National Center for Inter-university Research Facilities (NCIRF) at Seoul National University. X-ray diffraction (XRD) patterns were collected by Rigaku Smartlab X-ray diffractometer equipped with a Cu target and HyPix-3000 detector. Neutron powder diffraction data were collected on the high-resolution powder diffractometer Echidna [1] with neutron wavelength of 1.541 Å. Rietveld refinements of ND patterns were conducted using the TOPAS software. Field emission scanning electron microscopy (FE-SEM) images were obtained on an AIS 2000C scanning electron microscope.

Electrochemical evaluation of cathodes

The cathode materials are mixed with a carbon additive (acetylene black), binder (KF1100, Kureha corporation), and N-Methylpyrrolidone (Sigma-Aldrich) by mortar and pestle to prepare a slurry. The ratio of active material, carbon additive, and binder is 92:1:7. The slurries are cast on the Al foil by a doctor blade and dried for 5 hours in a vacuum oven at 120 ^{o}C. The average areal loading of electrodes was c.a. 10 mg cm^{-2}. The electrodes are cut into 12 cm^2 sized rectangle shape, and pouch cells are used for the electrochemical test. 200 μL of 1.3 M $LiPF_6$ in EC:DEC (1:1 vol.%) and polypropylene separator (Celgard) was used for the cell fabrication. Galvanostatic charge-discharge tests of the cells were performed with a current density of 30 mA g^{-1}.

Ex-situ resonant inelastic X-ray scattering (RIXS)

The O *K*-edge RIXS spectra were collected by iRIXS endstation at beamline 8.0.1 in Advanced Light Source, Lawrence Berkeley National Laboratory. The ultra-high efficient RIXS spectrometer helps the measurement of RIXS spectra without excessive damage to samples. A homemade transfer kit was used to transfer the species from the Ar-filled glovebox to the measurement chamber to avoid any air exposure to the samples. The RIXS spectra were continuously scanned through the O-*K* pre-edge region with the excitation energy step size of 0.2 eV and dwelling time of 90 seconds. To minimize beam damage, the specimen was repeatedly moved up and down by 0.5 mm during measurement, and it was confirmed that the spectrum was well averaged due to the long dwelling time. A systematic study shows the moving sample during the measurement effectively relieves the beam damage of the samples.[2] The collected spectra were fabricated to 2D RIXS maps as functions of emission and excitation energies. Further processing, including normalization, cosmic ray removal, etc., has been conducted for the 2D map.

X-ray Absorption Spectroscopy (XAS)

The Ni and Co L_3-edge XAS spectra were collected by iRIXS endstation at beamline 8.0.1 in Advanced Light Source, Lawrence Berkeley National Laboratory. The species are transferred in the same way as used for the RIXS experiments. The iRIXS endstation has two channels to collect the total fluorescence yield (TFY) and total electron yield (TEY), and both TFY and TEY signals are collected simultaneously.

Inverse partial fluorescence yield (iPFY)

Mn-L_3 iPFY was extracted through the formula iPFY = a/PFY_O, where a is a normalization coefficient, PFY_O is extracted by integrating the fluorescence intensity within the O-*K* emission energy range (490 to 530 eV) on the Mn-L_3 mRIXS. Mn-L_3 iPFY was used in this work instead of TFY to avoid the distortion observed in the conventional TFY caused by emission signals from oxygen.

Operando electrochemical mass spectroscopy (OEMS)

Electrode preparation for OEMS experiments

NCM electrodes for *operando* gas measurements were prepared by grinding NCM, acetylene black (Alfa Aesar, 50 % compressed, S.A. 75 $m^2 g^{-1}$, bulk density 80–120 g L^{-1}, 99.9%+) and polyvinylidene difluoride (Solvay, Solef 6010/1001) in an 85:8:7 mass ratio with an agate mortar and pestle inside an argon-filled glovebox (O_2 and H_2O <1 ppm). N-methyl-2-pyrrolidone (NMP, 99.5%, anhydrous, Sigma-Aldrich) was added to form a slurry, which was drop-cast onto stainless-steel mesh discs (12 mm ⌀; 1.13 cm^2). The electrodes were dried first at 60 °C for 2 hours and then at 120 °C under vacuum overnight. The active material loading was 3.5 – 4.5 mg cm^{-2}.

OEMS experiments

For the operando gas measurements, a custom-built setup and gas-tight cell, which have been described in detail in previous publications, [3-5] were used.

Custom Swagelok cells were assembled inside an argon-filled glovebox as follows: a lithium foil disc (12 mm ⌀), a quartz microfiber separator (Whatman, QM-A; 12.7 mm ⌀) wetted with 80 µL of electrolyte solution, an NMC electrode on stainless-steel mesh current collector (12 mm ⌀), a stainless-steel mesh disc (12 mm ⌀) and a stainless-steel ring spacer (12 mm ⌀) were compressed inside a modified Swagelok cell. The spacer ring creates a headspace (~100 µL) for gases to accumulate during battery operation. 1.5 M $LiPF_6$ in EC was chosen as the electrolyte solution for its low vapor pressure, thus contributing a smaller background signal in the mass spectra compared to electrolyte solutions containing linear alkyl carbonates.

After assembly, the NMC/Li cells were connected to the DEMS equipment and the headspace of the cell was filled with a positive argon pressure (~1.45 bar). During the electrochemical measurements, the cell headspace was flushed with 500 µL of argon by the DEMS instrument every 10 minutes, and any accumulated gases were swept to the mass spectrometer chamber for analysis. The mass spectrometer was calibrated for O_2 (research grade, Linde) and CO_2 (> 99.9%, Linde), allowing for the conversion of the ion current to partial pressure for O_2 and CO_2, which could then be used to quantify the gas formation using the ideal gas law (temperature and volume are known).

Electrochemical measurements were performed at 25 °C using a Biologic VSP potentiostat/galvanostat instrument running EC-lab software. After a 2-hour OCV period to establish a baseline value for all mass traces, the NMC/Li cells were cycled between 4.8 – 3.0 V_{cell}. Charging was performed at C/10 in constant current-constant voltage (CCCV) mode with a current limitation corresponding to C/100, and discharging was performed at C/5 in constant current (CC) mode.

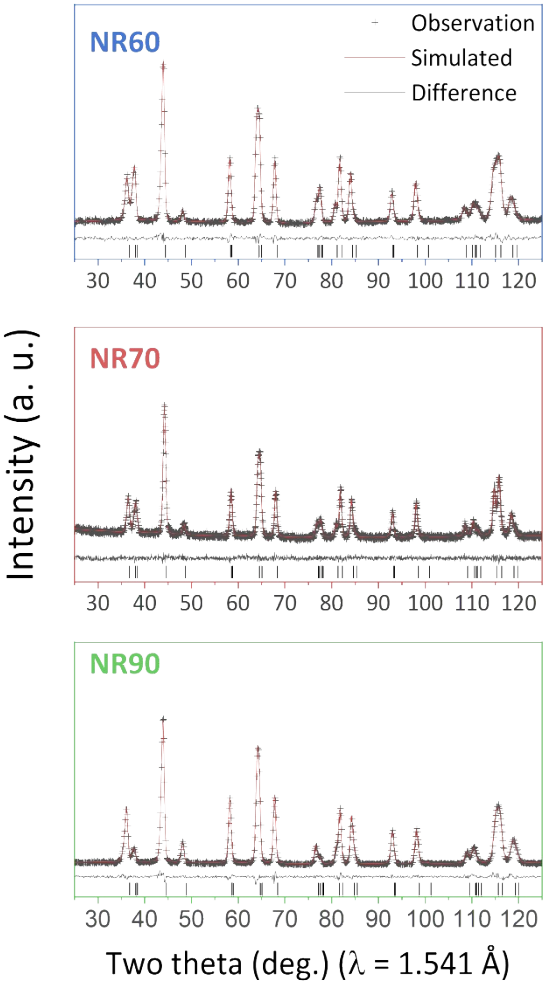

Fig. S1.
Rietveld refinement results of neutron diffraction patterns of NR-NCMs

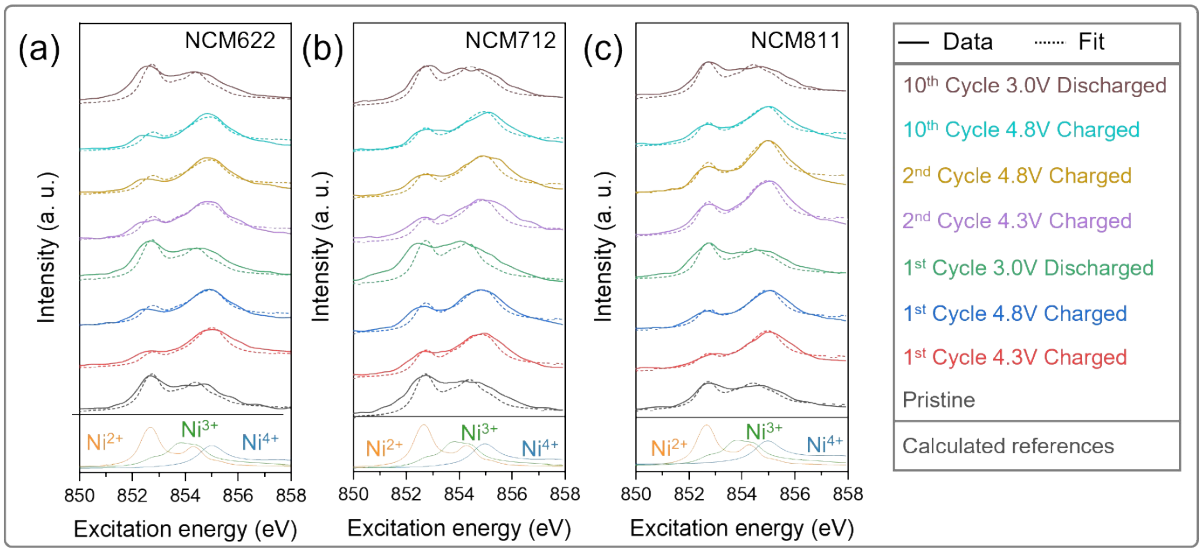

Fig. S2.

Ni-L_3 TFY analyses results of NR-NCMs. Soft X-ray absorption spectra of (A-C) Ni L_3-edge collected by total fluorescence yield (TFY) mode. Solid lines and dotted lines correspond to the experimental and fitted values, respectively. The fitted value is generated by the linear combination of the simulated $Ni^{2+/3+/4+}$ spectra plotted at the bottom of the boxes.

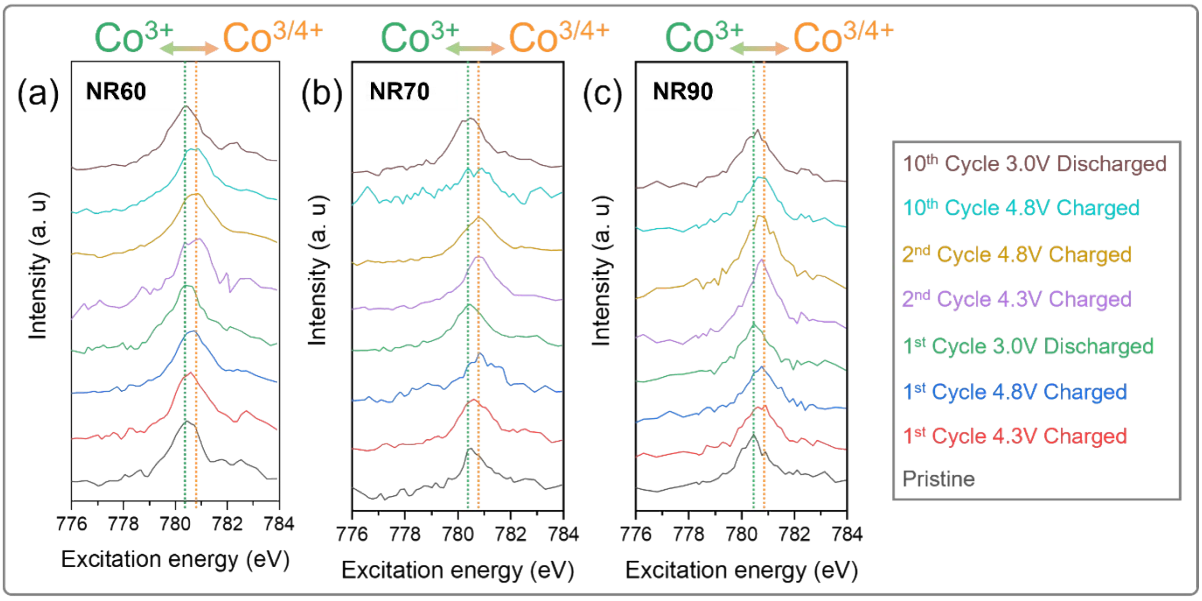

Fig. S3.

Co-L_3 TEY analyses results of NR-NCMs. Soft X-ray absorption spectra of a-c Co L_3-edge collected by total fluorescence yield (TFY) mode.

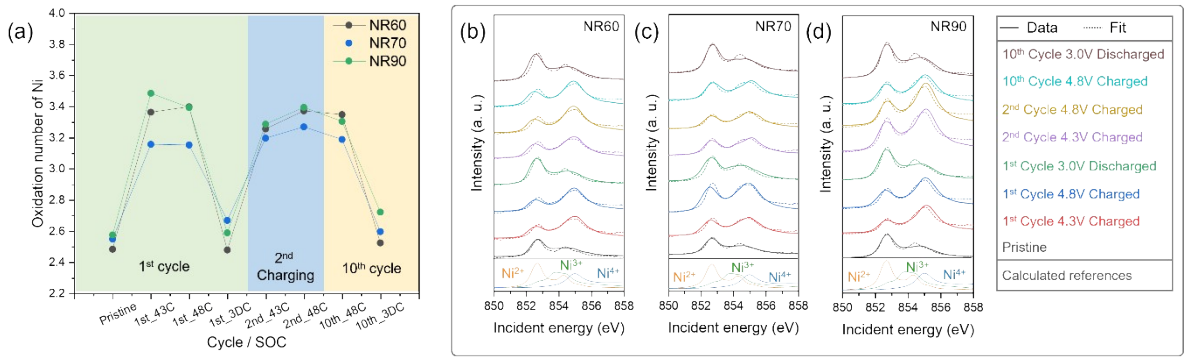

Fig. S4.

Ni-L_3 TEY analyses results of NR-NCMs. Soft X-ray absorption spectra of (a-d) Ni L_3-edge collected by total electron yield (TEY) mode. (a) Semi-quantitatively fitted Ni oxidation state trend extracted from Ni-L_3 spectra. (b-d) Solid lines and dotted lines correspond to the experimental and fitted values, respectively. The fitted value is generated by the linear combination of the simulated $Ni^{2+/3+/4+}$ spectra plotted at the bottom of the boxes.

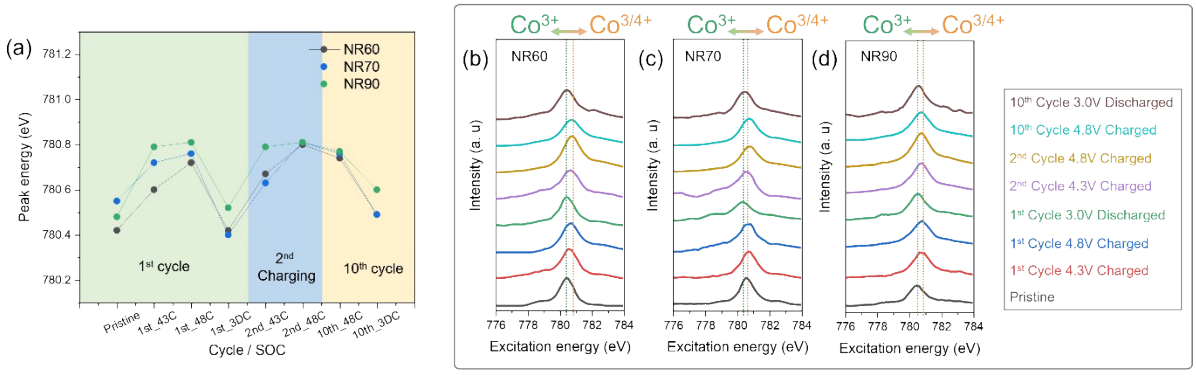

Fig. S5.

Co-L_3 TEY analyses results of NR-NCMs. Soft X-ray absorption spectra of (a-d) Co L_3-edge collected by total electron yield (TEY) mode. (a) Co peak energy trend during the cycling extracted from the (b-d) Co L_3-edge spectra.

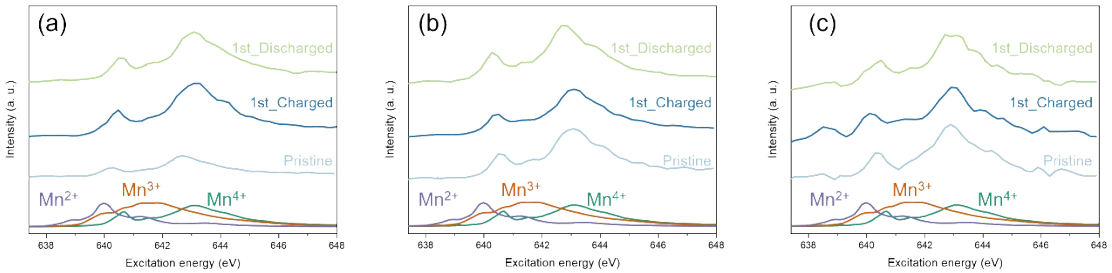

Fig. S6.

Mn-L_3 iPFY results of NR-NCMs. (a-c) The iPFY spectra extracted from mRIXS spectra for NR60, NR70, NR90, respectively. Each panel includes the spectra at states of charge of pristine, first full charged (4.8 V) and first discharged (3.0 V). The calculated reference spectra for Mn^{2+}, Mn^{3+} and Mn^{4+} were plotted together for the comparison. [1] The similarity of all spectra with Mn^{4+} reference indicates that Mn is kept to 4+ regardless of the material and the state of charge.

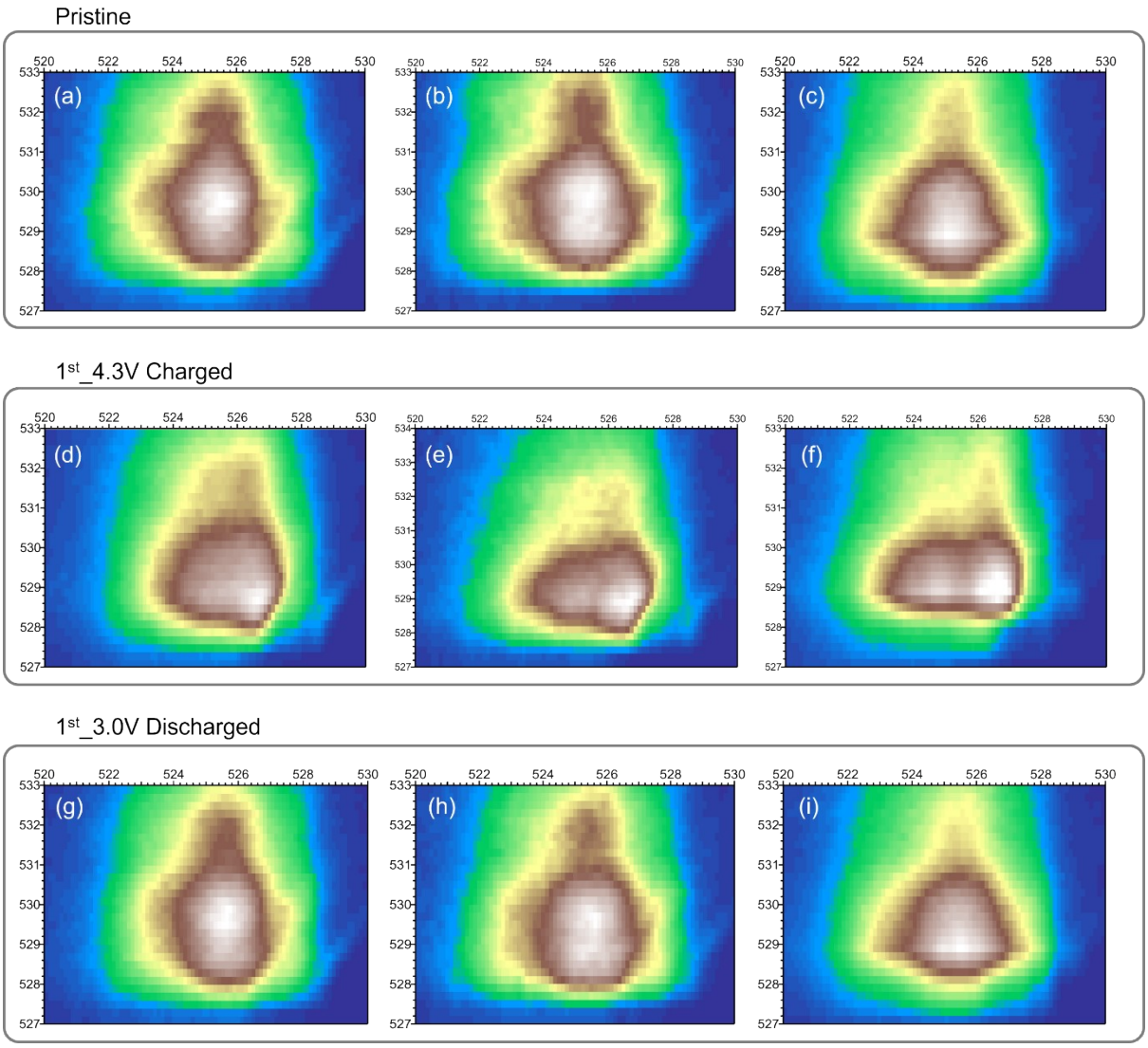

Fig. S7.

Additional mRIXS spectra of NR-NCMs at various states of charge: (a-c) Pristine, (d-f) first 4.3 V charged states and (g-i) first discharged states. (a, d, g) NR60, (b, e, h) NR70 and (c, f, i) NR90, respectively.

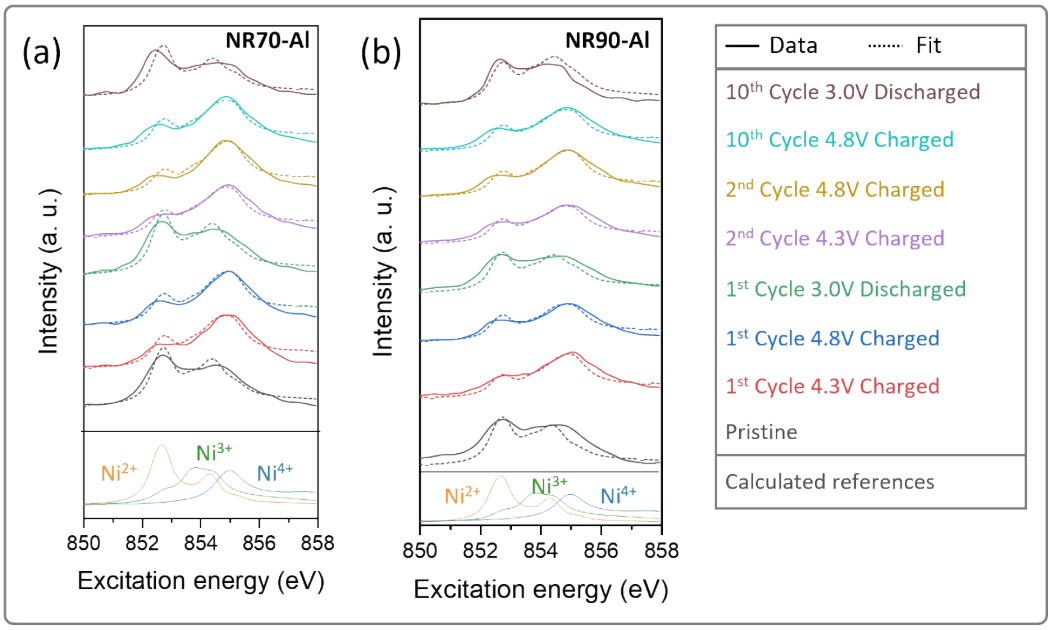

Fig. S8.

Ni-L_3 TFY analyses results of NR-NCMAs. Soft X-ray absorption spectra of **a, b** Ni L_3-edge collected by total fluorescence yield (TFY) mode. Solid lines and dotted lines correspond to the experimental and fitted values, respectively. The fitted value is generated by the linear combination of the simulated $Ni^{2+/3+/4+}$ spectra plotted at the bottom of the boxes.

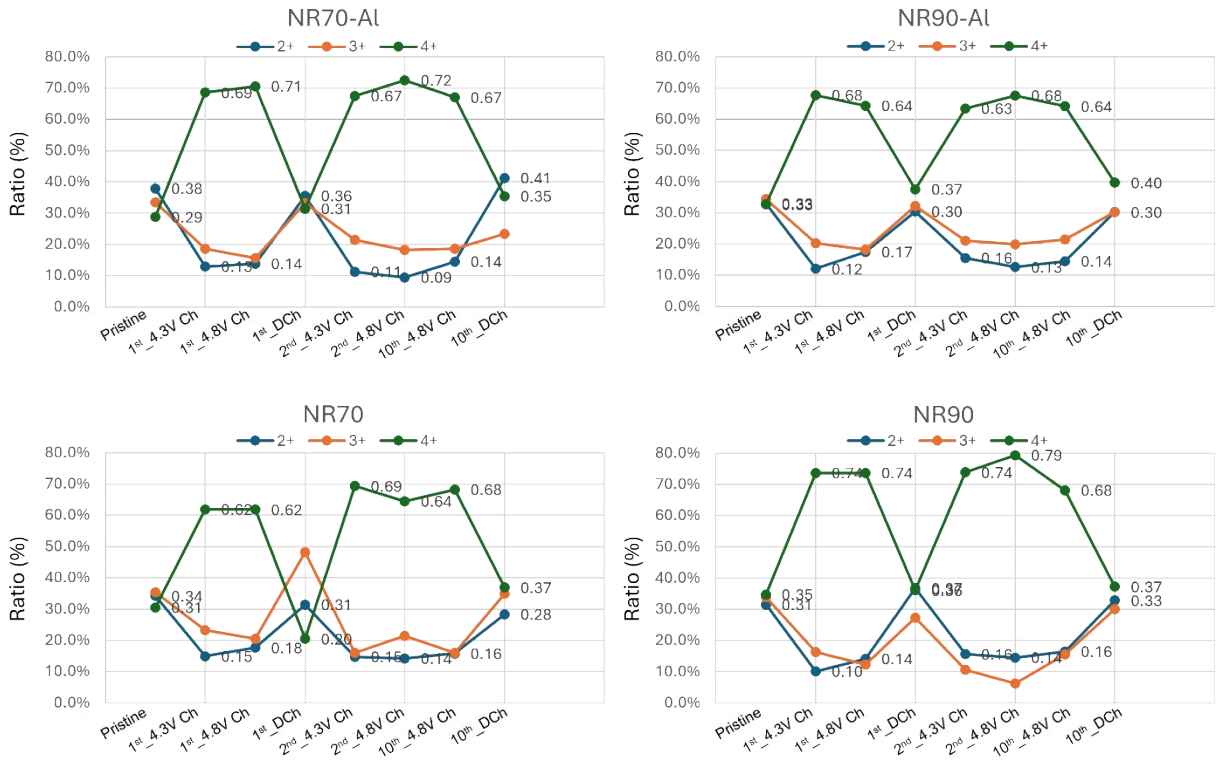

Fig. S9.

Ni oxidation state composition trends of NCM712/811 and NCMA712/811 from the linear combination fitting of spectra in Fig. S2 and S8.

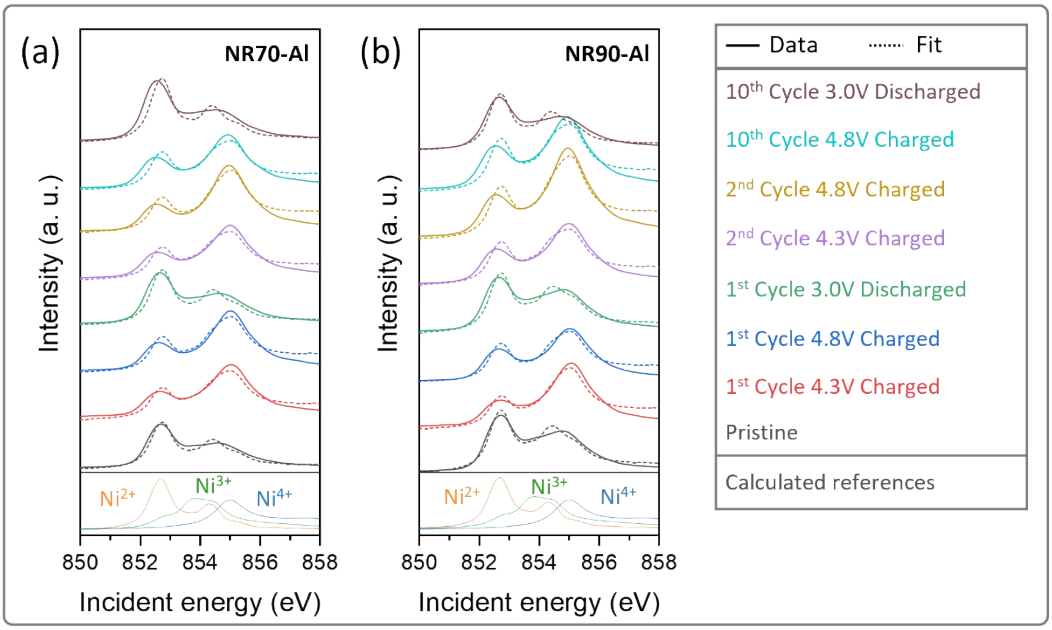

Fig. S10.

Ni-L_3 TEY analyses results of NR-NCMAs. Soft X-ray absorption spectra of **a, b** Ni L_3-edge collected by total fluorescence yield (TEY) mode. Solid lines and dotted lines correspond to the experimental and fitted values, respectively. The fitted value is generated by the linear combination of the simulated $Ni^{2+/3+/4+}$ spectra plotted at the bottom of the boxes.

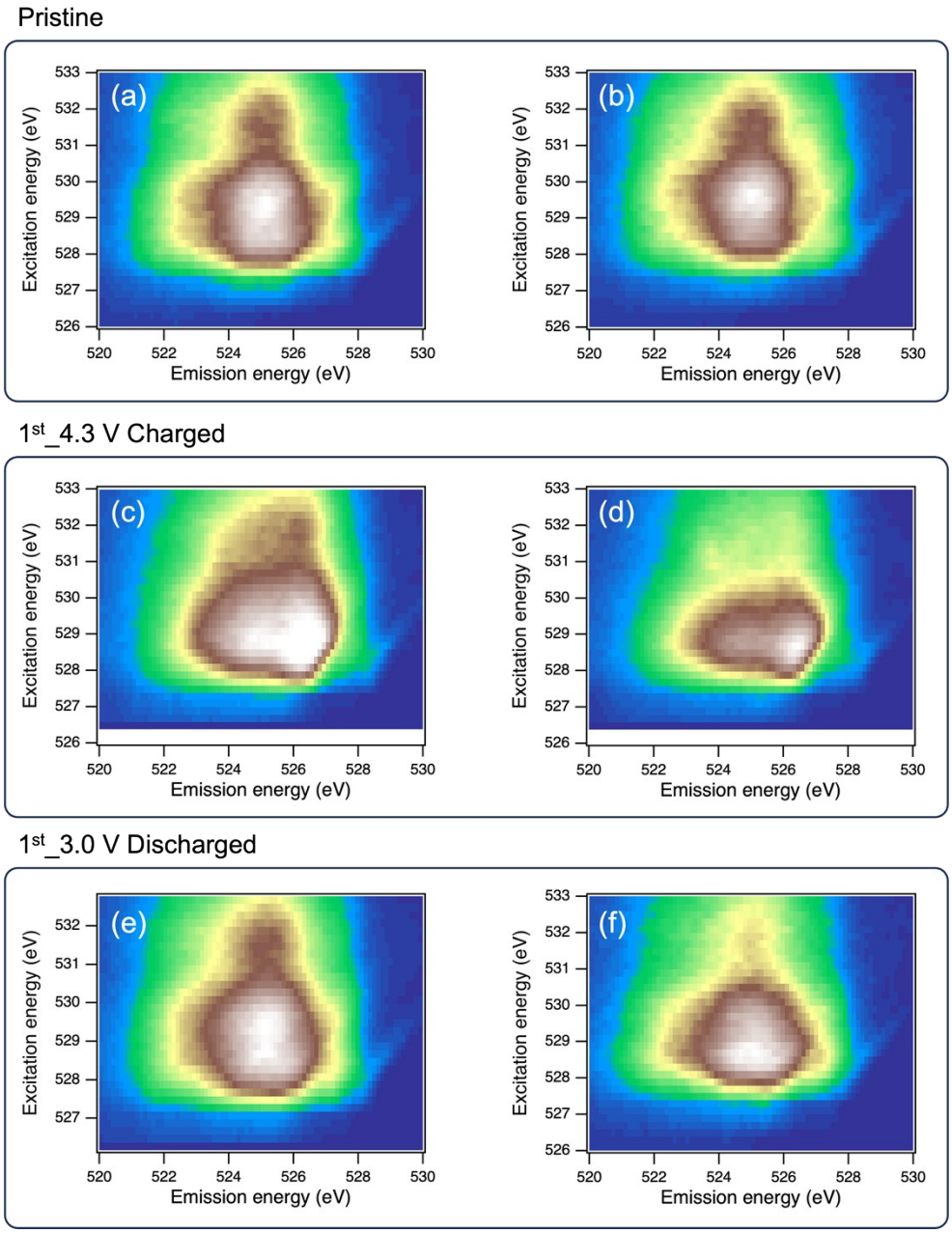

Fig. S11.

Additional mRIXS spectra of NR-NCMAs at various states of charge: (a, b) Pristine, (c,d) first 4.3 V charged states and (e, f) first discharged states. (a, c, e) NR70-Al, (b, d, f) NR90-Al, respectively.

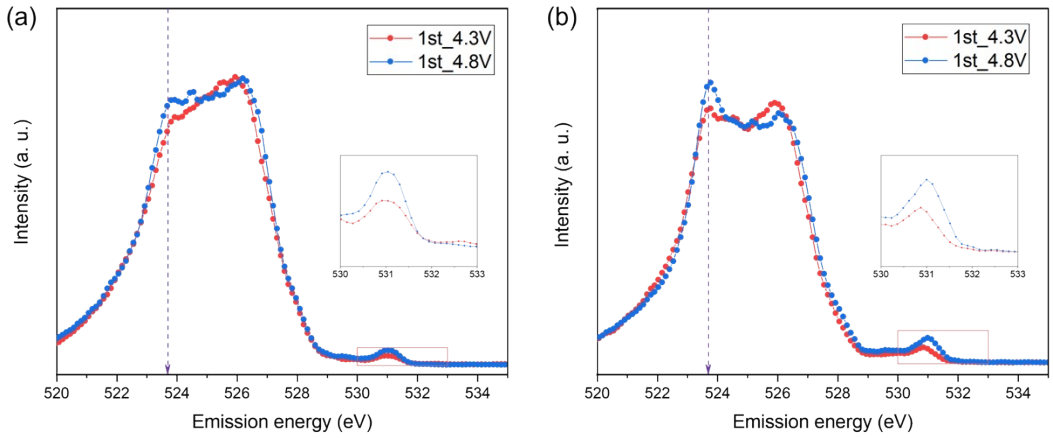

Fig. S12.

The summed O-*K* RIXS cuts of NR-NCMAs in the excitation energy of 530.9 – 531.3 eV at the first cycle with different voltage cut-offs. (a) NR70-Al (b) NR90-Al. The red box highlights the low energy emission features near the elastic lines arising from the oxygen redox.

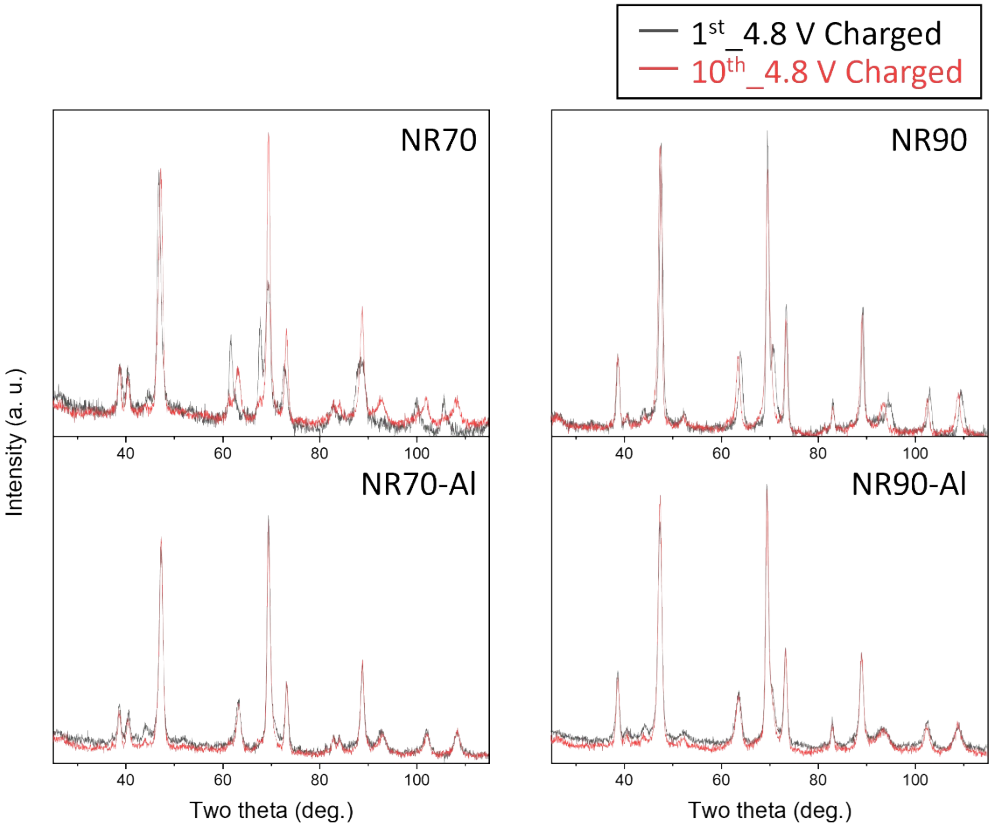

Fig. S13.

Full-range ND patterns of NR-NCMs & NR-NCMAs for the first and tenth charged states.

Samples	Elemental composition				
	Li	Ni	Co	Mn	Al
NR60	0.99	0.62	0.19	0.19	N/A
NR70	1.00	0.72	0.09	0.19	N/A
NR70-Al	0.98	0.73	0.09	0.19	0.007
NR90	0.97	0.87	0.1	0.06	N/A
NR90-Al	0.98	0.89	0.05	0.07	0.019
*Similar levels of impurities (> 2000 ppm) like Zr and B are detected through all samples					

Table S1.
The elemental composition of NR-NCMs and NR-NCMAs analyzed by ICP-OES

NR60 (space group: $R\bar{3}m$)

R_{wp} = 3.67 %, R_e = 1.49 %, R_p = 2.99 %, S (= R_{wp}/R_e) = 2.46

Lattice parameters: a = b = 2.86797(15) Å, c = 14.2172(10) Å, α = β= 90°, γ= 120°

Atom	Site	x	y	z	Occupancy	B_{iso} (Å)
Ni	3a	0	0	0	0.576(2)	0
Co	3a	0	0	0	0.210(6)	0
Mn	3a	0	0	0	0.194(10)	0
Li	3a	0	0	0	0.020(12)	0
Li2	3b	0	0	0.5	1	0
O	6c	0	0	0.25881(10)	1	0

NR70 (space group: $R\bar{3}m$)

R_{wp} = 2.90 %, R_e = 2.24 %, R_p = 2.34 %, S (= R_{wp}/R_e) = 1.30

Lattice parameters: a = b = 2.87326(3) Å, c = 14.22389(19) Å, α = β= 90°, γ= 120°

Atom	Site	x	y	z	Occupancy	B_{iso} (Å)
Ni	3a	0	0	0	0.646(2)	0
Co	3a	0	0	0	0.102(6)	0
Mn	3a	0	0	0	0.161(10)	0
Li	3a	0	0	0	0.091(12)	0
Li2	3b	0	0	0.5	0.956	0
Ni2	3b	0	0	0.5	0.044(12)	
O	6c	0	0	0.25881(10)	1	0

NR70-Al (space group: $R\bar{3}m$)

R_{wp} = 3.86 %, R_e = 1.47 %, R_p = 3.17 %, S (= R_{wp}/R_e) = 2.63

Lattice parameters: a = b = 2.86568(19) Å, c = 14.1868(10) Å, α = β= 90°, γ= 120°

Atom	Site	x	y	z	Occupancy	B_{iso} (Å)

Ni	3a	0	0	0	0.671(1)	0
Co	3a	0	0	0	0.0787(9)	0
Mn	3a	0	0	0	0.2483(2)	0
Li	3a	0	0	0	0.0015(15)	0
Li2	3b	0	0	0.5	1	0
O	6c	0	0	0.25869(12)	1	0

NR90 (space group: $R\bar{3}m$)

R_{wp} = 4.66 %, R_e = 1.31 %, R_p = 3.77 %, S (= R_{wp}/R_e) = 3.56

Lattice parameters: a = b = 2.86320(20) Å, c = 14.1526(11) Å, α = β= 90°, γ= 120°

Atom	Site	x	y	z	Occupancy	B_{iso} (Å)
Ni	3a	0	0	0	0.804(2)	0
Co	3a	0	0	0	0.152(5)	0
Mn	3a	0	0	0	0.044(5)	0
Li	3a	0	0	0	0	0
Li2	3b	0	0	0.5	0.981(5)	0
Ni2	3b	0	0	0.5	0.019(5)	0
O	6c	0	0	0.25881(10)	1	0

NR90-Al (space group: $R\bar{3}m$)

R_{wp} = 3.92 %, R_e = 1.59 %, R_p = 3.10 %, S (= R_{wp}/R_e) = 2.47

Lattice parameters: a = b = 2.86973(0) Å, c = 14.22726(0) Å, α = β= 90°, γ= 120°

Atom	Site	x	y	z	Occupancy	B_{iso} (Å)
Ni	3a	0	0	0	0.788(4)	0
Co	3a	0	0	0	0.030(20)	0
Mn	3a	0	0	0	0.093(14)	0

Al	3a	0	0	0	0.0090(12)	0
Li2	3b	0	0	0.5	0.981(5)	0
Ni2	3b	0	0	0.5	0.019(5)	0
O	6c	0	0	0.25881(10)	1	0

Table S2.

Parameters from Rietveld refinement of neutron diffraction patterns of NR-NCMs and NR-NCMAs

NR60	O_2 (μmol g^{-1})	CO_2 (μmol g^{-1})
Cycle 1	2.0041	104.3826
Cycle 2	0.2671	68.11

NR70	O_2 (μmol g^{-1})	CO_2 (μmol g^{-1})
Cycle 1	1.9817	113.3374
Cycle 2	0.9077	75.7738

NR70-Al	O_2 (μmol g^{-1})	CO_2 (μmol g^{-1})
Cycle 1	1.4933	84.3190
Cycle 2	0.5023	58.1831

NR90	O_2 (μmol g^{-1})	CO_2 (μmol g^{-1})
Cycle 1	1.5739	118.7847
Cycle 2	0.4572	72.9226

NR90-Al	O_2 (μmol g^{-1})	CO_2 (μmol g^{-1})
Cycle 1	1.2073	81.9391
Cycle 2	0.3577	53.0161

Table S2.

Accumulated CO_2/O_2 gas evolution during the cycling of NR-NCMs and NR-NCMAs

References

1. M. Avdeev and J. R. Hester, *J. Appl. Crystallogr.*, 2018, **51**, 1597-1604.
2. Q. Li, Z. W. Lebens-Higgins, Y. Li, Y. S. Meng, Y.-D. Chuang, L. F. J. Piper, Z. Liu and Wanli Yang, *J. Phys. Chem. Lett.*, 2021, 1**2**, 1138-1143.
3. B. D. McCloskey, R. Scheffler, A. Speidel, D. S. Bethune, R. M. Shelby and A. C. Luntz, *J. Am. Chem. Soc.*, 2011, **133**, 18038-18041.
4. B. D. McCloskey, D. S. Bethune, R. M. Shelby, G. Girishkumar and A. C. Luntz, *J. Phys. Chem. Lett.*, 2011, **2**, 1161-1166.
5. B. D. McCloskey, A. Valery, A. C. Luntz, S. R. Gowda, G. M. Wallraff, J. M. Garcia, T. Mori and L. E. Krupp, *J. Phys. Chem. Lett.*, 2013, **4**, 2989-2993.